Robotica (2001) volume 19, pp. 209–215. Printed in the United Kingdom © 2001 Cambridge University Press

Optimal input design for a cooperating robot to reduce vibration when carrying flexible objects

Young-Chun Ji and Youn-sik Park

Center for Noise and Vibration Control, Department of Mechanical Engineering, Korea Advanced Institute of Science and Technology, Science Town, Taejon 305–701 (Korea). E-mail: yspark@mail.kaist.ac.kr

(Received in Final Form: June 25, 2000)

SUMMARY

This paper presents a computational method for obtaining an optimal control trajectory for point-to-point motion of a cooperating robot carrying a flexible object. To increase the overall productivity and its efficiency, it is required to move the object as fast as possible using the maximum capacity of actuators of robots. If the carrying object is very sensitive to vibration, the robots should be operated so as not to cause excessive vibration of that object. This work deals with optimal input design for cooperative robots to reduce vibration of flexible objects that are handled at speed, under firm constraints on control torques.

KEYWORDS: Cooperating robots; Reduced vibration; Flexible objects; Input design; Fast motion.

1. INTRODUCTION

Robotic manipulation of flexible materials poses some new and challenging control problems and generates a growing interest due to its potential applications in industries such as assembly lines of automobiles. To enhance the overall productivity and its efficiency, one of the important issues is the optimization of some performance measures subject to the maximum capacity of actuators. This work presents a method for generating an optimal input during fast handling of flexible objects for raising productivity and, at the same time, reducing vibration during its motion.

In the last decade, multi-robotic systems have attracted extensive attention and a considerable amount of work has been published. Most of all the past work deals with cooperating robot system carrying a rigid object, but there are some cases of handling deformable flexible objects in the real world. Some researches present optimal force distribution of multiple cooperating robots carrying rigid objects,[1,2] time optimal motion for cooperating multiple rigid robot systems,[3,4] and etc. Others used feedback control to suppress the vibration of flexible objects.[5–7] Some publications deal with a simple PD position feedback,[8] PD plus gravity compensation[9,10] for controlling the position, orientation of a beam and a general flexible object manipulated by two robots. Also some publications are devoted to optimal input design of minimum time trajectory planning for a two-link rigid robot.[11–13]

This work deals with a cooperating robot carrying a flexible object from one position to another. In this case, the initial and final configurations are given and used as boundary conditions. Because joint torques are bounded in reality, it is assumed that those are constrained by certain lower and upper bounds. Flexible coordinates are included in the equation of motion. In order to obtain an optimal input for cooperating robots dealing with flexible object, an optimal control scheme[11] was used. Generally, the performance index includes carrying time, consuming energy and its level of vibration. Time is included to move the object as fast as possible, energy is considered to minimize its moving effort, and vibration is taken to suppress the unwanted motion during the working period. As mentioned above, constraints are set as the lower and the upper limits of a joint actuator torque. Boundary conditions are given as the configurations at the initial and final time. Using optimal control theory, two point boundary value problems (TPBVP) can be derived under these conditions. Several methods are known to solve this type TPBVP. Here, time normalization and variation of the externals method[14] are used. A good initial guess of the parameters is very important for solving this type TPBVP. In this work, a continuation technique which is adequate for a highly nonlinear system, was employed. In this method, a sequence of problems is solved, one for each choice of the continuation parameters, starting from a simpler one. At each stage, the unknown parameters calculated from the previous stage are used as the initial starting values of the parameters at the current stage.

It is assumed that two robots rigidly grasp a flexible beam and its motion is on a horizontal plane so as to neglect the gravity terms. In Section 2, a kinematics and dynamics equation of the system is constructed. Optimal control theory is briefly presented in Section 3. In Section 4, some simulations are done for a cooperating robot. Finally, a conclusion is presented.

2. COOPERATING ROBOT CARRYING A FLEXIBLE BEAM

2.1 Kinematics of the flexible beam and cooperating robots

A flexible uniform beam with length l is rigidly grasped by two planar robots having three revolute joints. Without loss of generality, a beam under free-free boundary condition (Figure 1) is considered. The transverse deflection and slope are approximated by a finite series of assumed modes,

https://doi.org/10.1017/S0263574700002915 Published online by Cambridge University Press

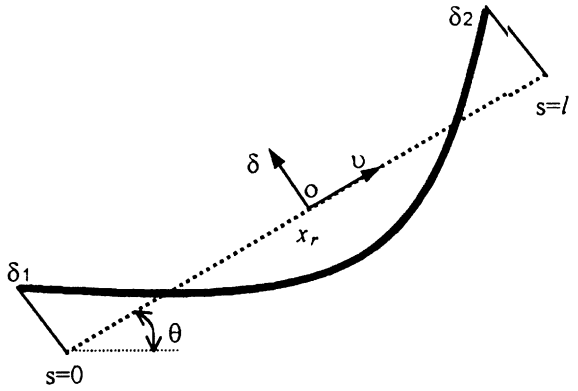


Fig. 1. Flexible beam under free-free boundary conditions.

$$\begin{aligned} &\delta = \mathbf{\Phi}(s)^T\eta(t) \quad \mathbf{\Phi}(s) = \{\phi_1(s) \ldots \phi_{N_m}(s)\}^T \\ &\delta' = \mathbf{\Phi}'(s)^T\eta(t) \quad \mathbf{\Phi}'(s) = \{\phi_1'(s) \ldots \phi_{N_m}'(s)\}^T \\ &\quad where,\ \eta = \{\eta_1 \ldots \eta_{N_m}\}^T : \text{set of flexible coordinates} \end{aligned} \tag{1}$$

where s denotes the spatial coordinate of the rigid beam and is in the range of 0 to l, $\phi_k(s)$ and $\phi_k'(s) = d\phi_k(s)/ds$ is a mode function and its derivative. $\eta_k(t)$ denotes the generalized flexible coordinate and N_m is the number of modes. The motion of a moving object, a beam, comprises as its rigid motion and elastic vibration. Rigid motion is described by $\mathbf{x}_r$ (3×1 vector), the position and orientation of the rigid beam. To describe its whole motion, a mobile coordinate frame o-$\upsilon\delta$ is attached to the beam, where the origin o is located at the mass center of the rigid beam. In the mobile frame, υ denotes the spatial coordinate of the rigid beam and is in the range $[-l/2, l/2]$. The rigid motion is represented by the motion of the mobile coordinate frame w.r.t. the inertial reference frame, and its elastic deformation is modeled as the relative displacement w.r.t. the mobile coordinate frame.

Let $\mathbf{x}_{e1}$ and $\mathbf{x}_{e2}$ (3×1) vectors represent positions and orientations of the two end-effectors respectively. Then the following relationships can be established:

$$\mathbf{x}_e = \{\mathbf{x}_{e1}^T,\ \mathbf{x}_{e2}^T\}^T = kin(\mathbf{x}_b) \quad where,\ \mathbf{x}_b = \{\mathbf{x}_r^T,\ \eta^T\} \tag{2}$$

$$\mathbf{x}_{e1} = \mathbf{x}_r - \left\{\frac{l\cos\theta}{2},\ \frac{l\sin\theta}{2},\ 0\right\}^T + \{-\delta_1\sin\theta,\ \delta_1\cos\theta,\ \delta_1'\}^T \tag{2a}$$

$$\mathbf{x}_{e2} = \mathbf{x}_r + \left\{\frac{l\cos\theta}{2},\ \frac{l\sin\theta}{2},\ \pi\right\}^T + \{-\delta_2\sin\theta,\ \delta_2\cos\theta,\ \delta_2'\}^T \tag{2b}$$

$$where,\ \delta_1 = \mathbf{\Phi}^T(0)\eta \quad \delta_1' = \mathbf{\Phi}'^T(0)\eta \qquad \delta_2 = \mathbf{\Phi}^T(l)\eta \quad \delta_2' = \mathbf{\Phi}'^T(l)\eta$$

Differentiating equation (2) one obtains

$$\dot{\mathbf{x}}_e = \mathbf{T}_b(\mathbf{x}_b)\dot{\mathbf{x}}_b \tag{3}$$

2.2 Dynamics of a cooperating robot

The dynamic equations of two robots (Figure 2) can be presented in the work space

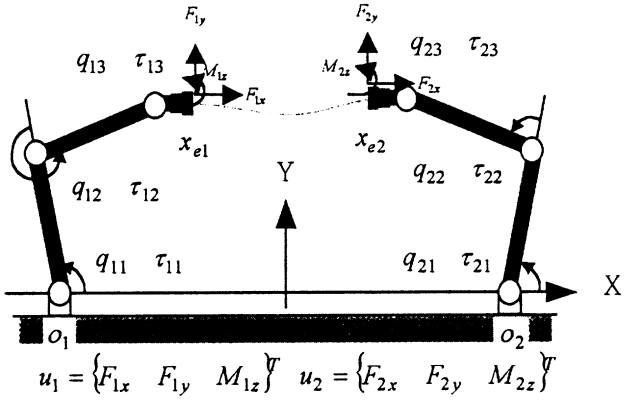


Fig. 2. Two cooperating robots.

$$\mathbf{A}(\mathbf{q})\ddot{\mathbf{q}} + \mathbf{b}(\mathbf{q}, \dot{\mathbf{q}}) = \tau + \mathbf{J}^T(\mathbf{q})\mathbf{u} \tag{4}$$

where $\mathbf{A}(\mathbf{q}) \in \Re^{6\times6}$ denotes the inertial matrix of robots. $\mathbf{b}(\mathbf{q}, \dot{\mathbf{q}}) \in \Re^{6\times1}$ is a nonlinear term. $\tau \in \Re^{6\times1}$ is the input of the robots. $\mathbf{J}(\mathbf{q}) \in \Re^{6\times6}$ is the Jacobian of robots and $\mathbf{u} = \{\mathbf{u}_1^T, \mathbf{u}_2^T\}^T \in \Re^{6\times1}$ denotes the interaction force exerted on the two end-effectors due to the carrying beam. Then the equation of motion for the beam can be written

$$\mathbf{M}\ddot{\mathbf{x}}_b + \mathbf{h}(\mathbf{x}_b, \dot{\mathbf{x}}_b) + \mathbf{K}\mathbf{x}_b = -\mathbf{T}_b^T(\mathbf{x}_b)\mathbf{u} \tag{5}$$

$\mathbf{J}(\mathbf{q})\dot{\mathbf{q}}$ is a Cartesian vector representing the velocity of the end effectors. Thus, from equation (3)

$$\mathbf{T}_b\dot{\mathbf{x}}_b = \mathbf{J}\dot{\mathbf{q}} \tag{6}$$

The time derivative of equation (6) yields

$$\ddot{\mathbf{q}} = \mathbf{J}^{-1}(\mathbf{T}_b\ddot{\mathbf{x}}_b + \dot{\mathbf{T}}_b\dot{\mathbf{x}}_b - \dot{\mathbf{J}}\dot{\mathbf{q}}) \tag{7}$$

under the assumption that no singular point exists. Substituting equations (4) and (7) into equation (5), yields

$$\begin{aligned} &\hat{\mathbf{M}}\ddot{\mathbf{x}}_b + \hat{\mathbf{h}}_b + \mathbf{K}\mathbf{x}_b = \mathbf{T}_b^T\mathbf{J}^{-T}\tau \\ &\quad where,\ \hat{\mathbf{M}} = \mathbf{M} + \mathbf{T}_b^T\mathbf{J}^{-T}\mathbf{A}\mathbf{J}^{-1}\mathbf{T}_b \\ &\qquad \hat{\mathbf{h}}_b = \mathbf{h}_b + (\mathbf{T}_b^T\mathbf{J}^{-T}\mathbf{A}\mathbf{J}^{-1}(\dot{\mathbf{T}}_b\dot{\mathbf{x}}_b - \dot{\mathbf{J}}\dot{\mathbf{q}}) + \mathbf{T}_b^T\mathbf{J}^{-T}\mathbf{b}) \end{aligned} \tag{8}$$

Equation (8) states that the joint angles and velocities can be specified with $\mathbf{x}_b$ and $\dot{\mathbf{x}}_b$ if no redundancy and singularities exist.

3. OPTIMUM INPUT DESIGN

3.1 Theory

Given a class of dynamic equations of the system, the control signals (if they exist) can be determined subject to some constraints that will move the system from any given initial state to the target state such that some performance index is minimized.

If $\mathbf{x} = \{\mathbf{x}_b^T, \dot{\mathbf{x}}_b^T\}^T$, equation (8) can be described by the state equation

$$\dot{\mathbf{x}}(t) = \mathbf{f}(\mathbf{x}(t)) + \mathbf{B}(\mathbf{x}(t))\,\tau(t) \tag{9}$$

where the state vector $\mathbf{x}(t) \in \Re^n$, $\mathbf{f}(\mathbf{x}) \in C^1(\Re^n,\ \Re^n)$, $\mathbf{B}(\mathbf{x}) \in C^1(\Re^n,\ \Re^{n\times m})$ and the control vector $\tau(t) \in \Re^m$. $n = 2(3 + N_m)$ and $m = 6$, where N_m is the number of considered modes of the beam. Equation (9) applies from initial state $\mathbf{x}_0$ to final target $\mathbf{x}_f$. The joint torques are constrained as

https://doi.org/10.1017/S0263574700002915 Published online by Cambridge University Press

$$\Omega = \{\tau(t) : L_i \le \tau_i(t) \le U_i \; i = 1, 2, \ldots, m, \forall t \in [0, T]\} \quad (10)$$

The performance index J, which is to be minimized with respect to the control vector $\tau(t)$, is

$$J = \int_0^{T_f} g(\mathbf{x}(t))dt \quad (11)$$

where, $g(\mathbf{x}(t)) \in C^1(\Re^n, R)$ and terminal time T_f is free.

In order to move a flexible object fast and at the same time suppress vibration during the motion, it is appropriate to set the performance index J, equation (11), to be

$$J = \int_0^{T_f} (1 + \frac{1}{2}\alpha\eta^T(t)\mathbf{R}_\eta\eta(t))\,dt \quad (12)$$

where α is a perturbation parameter and $\mathbf{R}_\eta$ (≥ 0) is diagonal weighting square matrix. If equation (12) is used as a performance index and there is not a singular interval, optimal control becomes one of a bang-bang type. But it is very difficult to obtain bang-bang control for a highly nonlinear system. Also bang-bang control can not be realized in a practical manner. In order to obtain a more smooth and practically applicable optimal input, the performance index J can be modified from equation (12) to equation (13) by adding an input energy term, $\frac{1}{2}\varepsilon\tau^T(t)\mathbf{R}_\tau\tau(t)$.

$$J(\tau(t)) = \int_0^{T_f} (1 + \frac{1}{2}\alpha\eta^T(t)\mathbf{R}_\eta\eta(t) + \frac{1}{2}\varepsilon\tau^T(t)\mathbf{R}_\tau\tau(t))dt \quad (13)$$

where ε is a perturbation parameter and $\mathbf{R}_\tau$ (>0) is a diagonal weighting square matrix.

Taking the performance index J as equation (13), a set of necessary conditions for optimality are obtained from Pontryagin's principle:

$$\dot{\mathbf{x}}^* = \frac{\partial H(\mathbf{x}^*, \lambda^*, \tau^*)}{\partial\lambda} \quad \dot{\lambda}^* = -\frac{\partial H(\mathbf{x}^*, \lambda^*, \tau^*)}{\partial\mathbf{x}}$$
$$H(\mathbf{x}^*, \lambda^*, \tau^*) = \min_{\tau(t)\in\Omega} H(\mathbf{x}^*, \lambda^*, \tau) \quad (14)$$

where τ^* is an optimal control candidate, $\mathbf{x}^*$ and λ^* are the corresponding nominal optimal state and costate trajectories, respectively, and the Hamiltonian function becomes

$$H(\mathbf{x}, \lambda, \tau) = 1 + \frac{1}{2}\alpha\eta^T(t)\mathbf{R}_\eta\eta(t) + \frac{1}{2}\varepsilon\tau^T(t)\mathbf{R}_\tau\tau(t) + \lambda^T(\mathbf{f}(\mathbf{x}(t)) + \mathbf{B}(\mathbf{x}(t))\tau(t)) \quad (15)$$

Using the Pontriagin's minimum principle, an optimal control law can be achieved

$$\tau_i(t) = \begin{cases} U_i & \text{if } S_i(t) > U_i \\ L_i & \text{if } S_i(t) < L_i \\ S_i(t) & \text{if } L_i(t) \le S_i(t) \le U_i \end{cases} \quad \text{for } t \in [t_1, t_2] \subset [0, T_f] \quad (16)$$

where $S_i(t)$ is the i-th component of the $m \times 1$ switching function defined by

$$\mathbf{S}(t) = -\frac{1}{\varepsilon}\mathbf{R}_\tau^{-1}\mathbf{B}^T(\mathbf{x})\lambda(t) \quad (17)$$

The transversability condition, equation (18) which is used as boundary condition, should be satisfied.

$$H(T_f) = 0 \quad (18)$$

Intuitively it can be seen that as ε is progressively reduced towards zero, the solution of the perturbed optimal control problem approaches that of the original optimal control problem. In case that the vibration term is not included in the performance index, the convergence of the algorithm was mathematically proved and verified by numerical simulations.[12] This transformation enables us to use the existing TPBVP algorithms to obtain the optimal solutions.

3.2 Computational procedure

Unless the system is of low order, time invariant and linear, there is little hope of solving the TPBVP analytically.[14] Such problems may be solved numerically by a shooting method or by any other iterative procedure. In general, the shooting method and a variation of the extremals method was found to be highly sensitive to the initial setting of the costate values. In order to find a good initial guess of the costate values, a continuation technique can be employed.

Figure 3 shows how (ε, α) in equation (13) is changed to obtain a sub-optimal solution of equation (12). We need to obtain the solution at $(\varepsilon_0, 0)$ to progress the initial costates from $(\varepsilon_0, 0)$ to $(\varepsilon_f, \alpha_f)$. To obtain the optimal solution for a nonlinear and coupled system at $(\varepsilon_0, 0)$, the following steps 1–3, are performed. And following steps 4–6, are procedures to obtain the solution at $(\varepsilon_f, \alpha_f)$ from that of $(\varepsilon_0, 0)$. By introducing the continuation parameters $\mathbf{p} = \{p_1 \ldots p_{N_p}\}^T$ $(N_p \times 1)$, the original system is transformed into

$$\dot{\mathbf{x}}(t) = \mathbf{f}(\mathbf{x}(t), \mathbf{p}) + \mathbf{B}(\mathbf{x}(t), \mathbf{p})\tau(t) \quad (19)$$

The transformed system equation of the original one, equation (19) is used in the following steps 1–3.

Steps 1–6

1. Let $\mathbf{p} = 0$, initially, which means the coupling and nonlinear terms are zero. In this case, an optimal solution

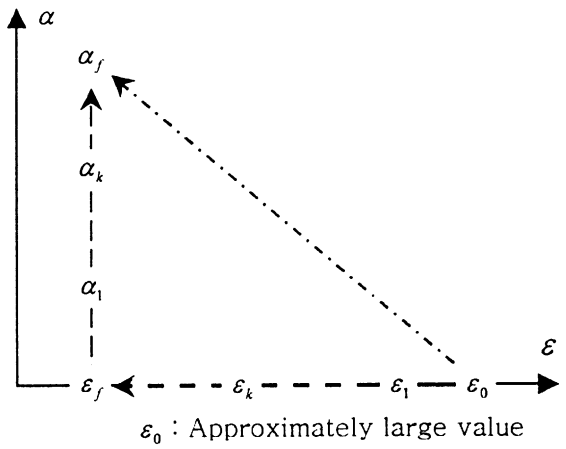


Fig. 3. Computational procedures in the ε–α plane.

https://doi.org/10.1017/S0263574700002915 Published online by Cambridge University Press

for the performance index, equation (13) can be easily obtained. With an appropriately large starting value of ε_0, TPBVP is solved.

2. Increasing p_1 from 0 toward 1 by an amount of reasonably small value, solve the TPBVP using the previous results as new initial guesses.
3. Repeat Step 2 for p_i, $i = 2$, N_p. Finally, $\mathbf{p} = \mathbf{1}$, that is, the solution to the complete nonlinear and coupled system for the given ε_0 can be obtained.
4. Taking the previous results as a new initial guess for ε_{k+1} which is smaller than ε_k (k is initially 1.), solve the TPBVP again. Then set $k = k + 1$ and repeat this step until

$$\frac{\Delta T_f}{\Delta \varepsilon} \times \varepsilon_k \leq C_{T_f} \times T_{f,k} \tag{20}$$

is satisfied, where C_{T_f} is a constant value which is less than 1 and used as index for termination of convergency. As ε_k moves to 0, T_f converges to a certain value. If ε_k is sufficiently small and equation (20) is satisfied, $T_{f,k}$ is smaller than the value of $(1 + C_{Tf}) \times T_f$ where T_f is the minimum moving time.

5. Set ε_k to ε_f.
6. Using the results from Step 4 as a new initial guess, for α_{k+1} which is greater than α_k ($\alpha_0 = 0$, k is initially 0), solve TPBVP repeatedly. Then set $k = k + 1$ and repeat this step, until the change of vibration quantity $\int_0^{T_f} \frac{1}{2}\eta^T \mathbf{R}_\eta \eta dt$ is negligibly small while maintaining the value of ε as ε_f.

3.3 Variation of extremals method

A variation of the extremals method is used to solve a TPBVP. If we know $\mathbf{x}(0) = \mathbf{x}_0$, $\lambda(0) = \lambda_0$ and T_f, then $\mathbf{x}(T_f)$, $\lambda(T_f)$ and $H(T_f)$ can be calculated using an ordinary differential equation solver for the initial value problem. Because the boundary conditions are given such as

$$\mathbf{x}(0) = \mathbf{x}_0 \quad \mathbf{x}(T_f) = \mathbf{x}_f \quad H(T_f) = 0 \tag{21}$$

the nonlinear equations can be constructed as

$$\mathbf{y}(\mathbf{z}) = \begin{Bmatrix} \mathbf{x}(\mathbf{x}_0, \lambda_0, t)\big|_{t=T_f} - \mathbf{x}_f \\ H(\mathbf{x}(t), \lambda(t))\big|_{t=T_f} \end{Bmatrix} = 0 \tag{22}$$

where, $\mathbf{z} = \{\lambda_0^T, T_f\}^T$ is unknown. If the terminal time is free, and the state equation (9) and the performance index are not explicit functions of t, then $\dot{H}$ becomes zero. Thus equation (22) can be written as

$$\mathbf{y}(\mathbf{z}) = \begin{Bmatrix} \mathbf{x}(\mathbf{x}_0, \lambda_0, t)\big|_{t=T_f} - \mathbf{x}_f \\ H(\mathbf{x}(t), \lambda(t))\big|_{t=0} \end{Bmatrix} = 0 \tag{23}$$

To solve the ordinary differential equation, the IMSL routine DVERK was used. To solve the nonlinear equation (23), the modified Newton method[15] (coded by us), and continuation algorithm[16] (version 6.1 of PITCON, the University of Pittsburgh continuation program) were used in this work.

Table I. Flexible beam properties (rectangular cross section).

Property	Value
Width	$100mm$
Height	$4mm$
Young's Modulus	$200GPa$
Density	$8000Kg/m^3$
Length	$2m$

4. SIMULATIONS

In order to establish the applicability of the proposed method, two planar 3 DOF robots holding a rectangular flexible steel beam (Table I) were numerically tested. It is assumed that two robots are identical and all links of the robots (Table II) are uniform rigid beams. The robot actuator torques are bounded, such as $|\tau_{i1}| \leq 150Nm$, $|\tau_{i2}| \leq 100Nm$ and $|\tau_{i3}| \leq 50Nm$, where $i = 1, 2$. The base coordinates of the two robots are positioned at $\mathbf{o}_1 = (-1.5, 0)$ and $\mathbf{o}_2 = (1.5, 0)$. At the initial and final position, the rigid coordinates of the beam are set to $\mathbf{x}_r(0) = (0, 0.5, 0)$ and $\mathbf{x}_r(T_f) = (0, 1.5, 0)$ (Figure 4) and flexible coordinates are set to zero. Only the first mode of flexible beam is considered to calculate robot torques. The weighting matrices $\mathbf{R}_\eta$ and $\mathbf{R}_\tau$ in the performance index J, equation (13), are set to the identity matrix, respectively.

Simulations were done along the two different calculation paths (Figure 5). Path 1 is obtained as follows: In the first stage of the path 1, (ε, α) moves from point A to point B until equation (20) is satisfied. In the second stage of the path 1, (ε, α) moves along from point B to point C. Unlike path 1, path 2 is followed by changing ε and α simultaneously from point A to point C directly. From the simulation, it was found that the results from the two different paths are identical.

At the point B and C in Figure 5, the required joint torques for the first (left-side) robot are shown in Figures 6

Table II. Length and mass of first robot links.

Number of link	length	mass
1	$1m$	$10kg$
2	$1m$	$10kg$
3	$0.1m$	$1kg$

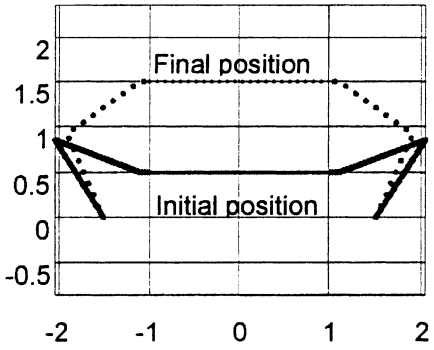


Fig. 4. Initial and final configuration of the manipulator system.

https://doi.org/10.1017/S0263574700002915 Published online by Cambridge University Press

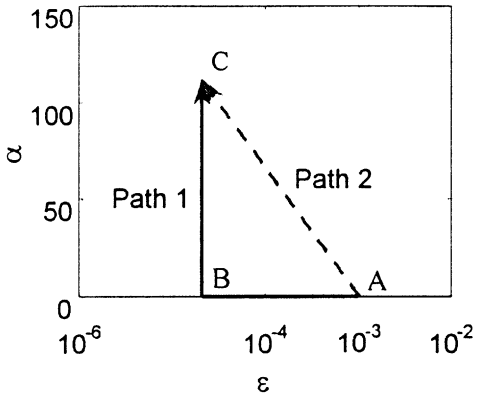


Fig. 5. Path of the chosen values of ε and α.

and 7. The torques of the second (right-side) robot is opposite in sign to the torques of the first robot. From the Figures 6 and 7, it can be seen that the constraints of the torques are all satisfied. Also it is observed that τ_{i3} ($i = 1, 2$) varies more than the other torques. This means that τ_{i3} are more related to beam vibration than the other actuators.

Figure 8 shows Y coordinate of the center of gravity of the beam. Figure 9 plots the beam vibration at the end-effectors. In Figures 8 and 9, the obtained torques, using the first mode of the beam, are applied to the system having 6 modes. In this work, the system having six modes is assumed as a real structure system. The vibarion at point C is more considerably reduced than that at point B. The residual vibration is greatly reduced at point *C*. The first natural frequency of the system at the final configuration is 2.2*Hz* and its residual vibration is dominated by the first natural frequency (Figure 9). Hence it can be said that if the obtained path can reduce its vibration during the motion, it can also curtail the residual vibration after the point-to-point motion. The maximum vibration level at the end-effectors is reduced by about 85% by including the vibration term in the performance index (Figure 9). Table III shows that there is an 11% increment in T_f, 44% increment in input energy and 98% reduction in vibration level at the point *C*, compared to

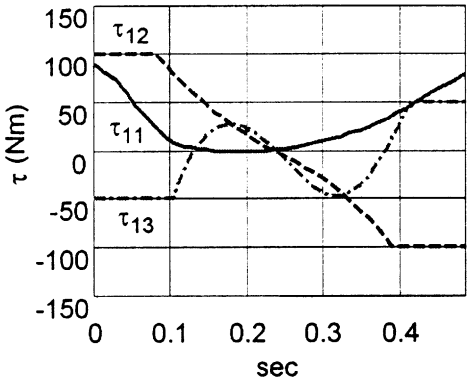


Fig. 6. Torques on the first (left-side) robot at point B.

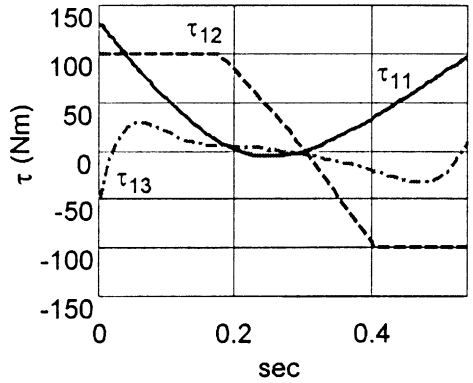


Fig. 7. Torques on the first (left-side) robot at point C.

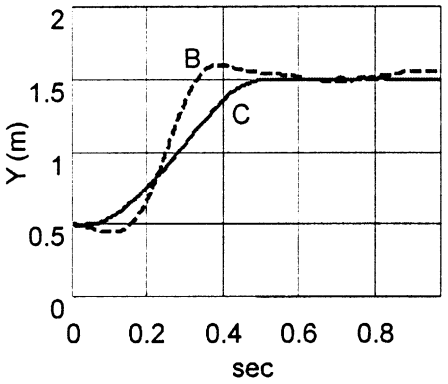


Fig. 8. *Y* coordinate of the center of gravity of the beam.

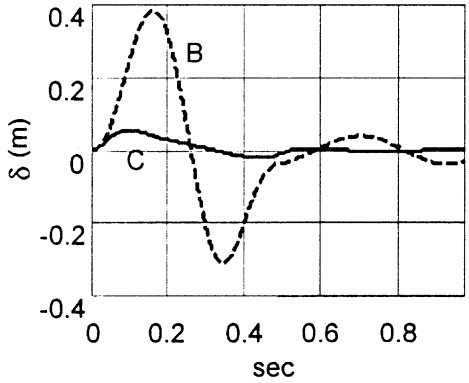


Fig. 9. Vibration at the end-effectors.

Table III. Terminal time, input energy and vibration quantity at the point A, B and C (cf. $(\varepsilon, \alpha) = (2.0535 \times 10^{-5}, 111.9)$ at C).

Point in Figure 5	A	B	C
Terminal time (T_f)	1.015	0.4865	0.5398
Input energy ($\int_0^{T_f} \frac{1}{2} \tau^T \mathbf{R}_\tau \tau dt$)	323.9	3959	5693
Vibration quantity ($\int_0^{T_f} \frac{1}{2} \eta^T \mathbf{R}_\eta \eta dt$)	1.532×10^{-3}	5.616×10^{-3}	1.044×10^{-4}

https://doi.org/10.1017/S0263574700002915 Published online by Cambridge University Press

those at point B. A relatively small variation in terminal time and input energy yields a considerably larger reduction in vibration quantity. Figures 10, 11 and 12 show the values of the terminal time, input energy and vibration quantity when the paths are used along the path 1. Figure 12 shows that even if α is greatly increased, there is just a little reduction in the vibration quantity.

The computational burden is heavy because this work solves two point boundary value problems; decreasing ε and increasing α. According to the simulation results, it was found that the reduction of vibration is very small when increasing the value of α greater than a certain value (Figure 12). But the computing effort becomes considerably heavier with the increasing value of α.

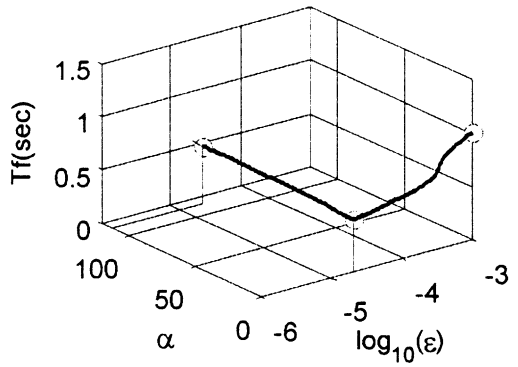


Fig. 10. Variation of terminal time, T_f, along the path 1.

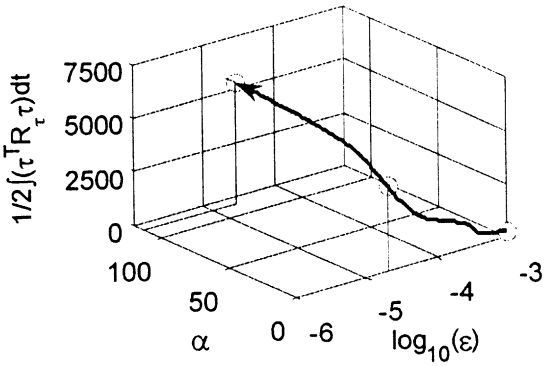


Fig. 11. Variation of input energy $\frac{1}{2}\int_0^{T_f}\tau^T\mathbf{R}_\tau\tau dt$, along the path 1.

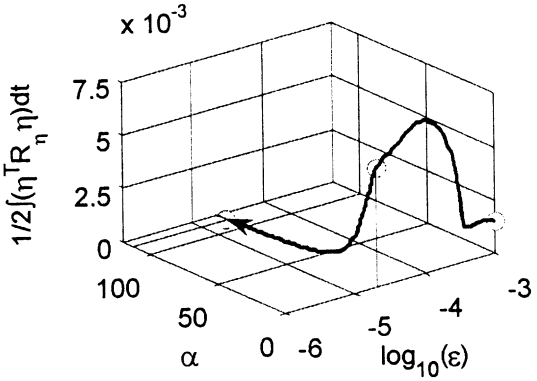


Fig. 12. Variation of vibration quantity, $\frac{1}{2}\int_0^{T_f}\eta^T\mathbf{R}_\eta\eta dt$, along the path 1.

5. CONCLUSIONS

This work presents a procedure to find an optimal input for point-to-point motions of cooperating robots carrying a flexible object. Because both the time and vibration quantity are included in the performance index, the obtained robot's path can deliver the flexible object fast enough while suppressing its vibration considerably during the motion. It is observed that the reduction of the vibration during the motion can result in a reduction of the residual vibration after motion ($t > T_f$) at the same time. It can be concluded that for a flexible system under the firm constraint of the actuators, an optimal trajectory giving less vibration and a fast motion time can be obtained using the proposed procedures.

References

1. W.S. Lu and W.H. Max Meng, "An Improved Load Distribution Scheme for Coordinating Manipulators", *Proceedings of the 1993 IEEE International Conference on Robotics and Automation* (1993) pp. 523–528.
2. Woong Kwon and Bum Hee Lee, "Optimal Force Distribution of Multiple Cooperating Robots using Nonlinear Programming Dual Method", *Proceedings of the 1996 IEEE International Conference on Robotics and Automation* (1996) pp. 2408–2413.
3. Young-Dal Shin, "Force Distribution and Minimum Time Trajectory Planning Using Generalized Weak Points on Cooperating Multiple Robot Manipulators", *PhD Thesis* (Department of Electrical Engineering, KAIST, 1992).
4. H.K. Cho, B.H. Lee and M.S. Ko, "Time-Optimal Motion of a Cooperating Multiple Robot System Along a Prescribed Path", *IEEE Transactions on Systems, Man, and Cybernetics* **25**, No. 12, 1648–1657 (1995).
5. T. Yukawa, M. Uchiyma and H. Inooka, "Cooperating Control of a Vibrating Flexible Object by a Rigid Dual-Arm Robot", *Proceedings of the 1995 IEEE International Conference on Robotics and Automation* (1995) pp. 1820–1826.
6. T. Yukawa, M. Uchiyma, D.N. Nenchev and H. Inooka, "Stability of Control System in Handling of a Flexible Object by Rigid Arm Robots", *Proceedings of the 1996 International Conference on Robotics and Automation* (1996) pp. 2332–2339.
7. Dong Sun and Yunhui Liu, "Modeling and Impedance Control of a Two-Manipulator System Handling a Flexible Beam", *Proceedings of the 1997 IEEE International Conference on Robotics and Automation* (1997) pp. 1787–1792.
8. Dong Sun, Yunhui Liu and James K. Mills, "Cooperative Control of a Two-Manipulator System Handling a General Flexible Object", *Proceedings of IEEE/RSJ International Conference on Intelligent Robots and Systems* (1997) pp. 5–10.
9. Dong Sun, James K. Mills and Yanhui Liu, "Position Control of Multiple Robots Manipulating a Flexible Payload", *Proceedings of the American Control Conference* (1998) pp. 456–460.
10. Dong Sun, James K. Mills and Yanhui Liu, "Position Control of Robot Manipulators Manipulating a Flexible Payload", *Int. J. Robotics Research*, 319–332 (1999).
11. Y. Chen and A.A. Desrochers, "Minimum-time control laws for robotic manipulators", *Int. J. Control* **57**, No. 1, 1–27 (1993).
12. Y. Chen and Jian Huang, "A Numerical Algorithm For Singular Optimal Control Synthesis Using Continuation Methods", *Optimal Control Applications and Methods* **15**, 223–236 (1994).
13. Y. Chen and Jian Huang, "An improved computation of time-optimal control trajectory for robotic point-to-point motion", *Int. J. Control* **65**, No. 1, 177–194 (1996).

https://doi.org/10.1017/S0263574700002915 Published online by Cambridge University Press

14. D.E. Kirk, *Optimal Control Theory An Introduction* (Prentice-Hall, Englewood Cliffs, NJ, 1970).
15. J. Stoer and R. Burlisch, *Introduction to Numerical Analysis* (Springer-Verlag, Berlin, 1980).
16. Eugene L. Allgower and Kurt Georg, *Numerical Continuation: Methods An Introduction* (Springer-Verlag, Berlin, 1990).

https://doi.org/10.1017/S0263574700002915 Published online by Cambridge University Press